Experimental study and modelling of a filtration–consolidation step: Towards the development of a design tool for cassava dewatering

Léa van der Werf, Alisia Chiadò Rana, Arnaud Chapuis, Charlotte Delpech, Christelle Wisniewski, Francis Courtois

Experimental study and modelling of a filtration-consolidation step: towards the development of a design tool for cassava dewatering

Léa van der Werf[a,b], Alisia Chiadò Rana[a,b], Arnaud Chapuis[a,b,c,*], Charlotte Delpech[a,b], Christelle Wisniewski[b] and Francis Courtois[b]

[a] *Cirad, UMR QualiSud, F-34398 Montpellier, France*

[b] *Qualisud, Univ Montpellier, Avignon Université, Cirad, Institut Agro, IRD, Université de La Réunion, Montpellier, France*

[c] *Cirad, UMR QualiSud, Saint-Louis, Sénégal*

ARTICLE INFO

Keywords:

Filtration

Consolidation

Modelling

Dewatering

Cassava

ABSTRACT

Dehydration is a critical step in many food processes. In this paper, we propose an original strategy, based on experiments and modelling, to evaluate the performance of the compression dewatering of cassava and to help design dewatering equipment. The dewatering of various grated cassava roots was experimentally studied through 42 experiments in a filtration-consolidation cell in the pressure range $4 - 21$ *bar*. The dewatering performance was evaluated in terms of moisture content limit and dewatering kinetics. Each filtration-consolidation experiment was first individually fitted with a model combining Hermia cake filtration and Shirato consolidation mechanisms using an original systematic approach. Then, a global model, linking the cake filtration and consolidation properties to the applied pressure, was validated over the whole set of experiments with an average RMSE of 13% on the cake moisture content. The results demonstrated the relevance of the chosen identification procedure and modelling strategy for the design of a compression dewatering step.

*Corresponding author: Arnaud Chapuis

lea.van_der_werf@cirad.fr (L. van der Werf); alisia.chiado_rana@cirad.fr (A. Chiadò Rana); arnaud.chapuis@cirad.fr (A. Chapuis); charlotte.delpech@cirad.fr (C. Delpech); christelle.wisniewski@umontpellier.fr (C. Wisniewski); francis.courtois@umontpellier.fr (F. Courtois)

ORCID(s): 0000-0002-2977-3504 (L. van der Werf); 0000-0002-8118-6518 (A. Chiadò Rana); 0000-0002-7833-2641 (A. Chapuis); 0000-0002-3068-5018 (C. Wisniewski); 0000-0002-6233-5397 (F. Courtois)

Nomenclature

A	filtration surface area $[m^2]$
C	volume fraction of solids in cake $[-]$
C_0	coefficient equal to the volume fraction of solids in cake at 1 bar $[bar^{-\beta}]$,
C_e	modified consolidation coefficient $[m^2 \cdot s^{-1}]$
C_{e0}	coefficient equal to the modified consolidation coefficient at 1 bar $[m^2 \cdot s^{-1} \cdot bar^{-\gamma}]$,
DM	mass fraction of dry matter on wet basis (w.b.) $[-]$
d_{50}	median diameter $[\mu m]$
i	number of drainage surfaces $[-]$
L	product height in the equipment $[m]$
m	mass $[kg]$
n	compressibility index in filtration $[-]$
P	pressure applied $[Pa]$ or $[bar]$ depending on the context
R_s	cloth filter resistance $[m^{-1}]$
t	time $[sec]$
T_c	dimensionless consolidation time $[-]$
U_c	consolidation ratio $[-]$
Vol	volume $[m^3]$
V_s	volume of solids in the press per filtration surface area $[m^3 \cdot m^{-2}]$
W	mass of deposited dry cake per unit of filtrate volume $[kg \cdot m^{-3}]$
X	mass fraction of water on wet basis (w.b.) $[-]$
Y	coefficient representing the product pressure-dependent properties in consolidation $[-]$
Y_0, Y_1	parameters of the correlation between Y and the applied pressure $[-]$

Greek letters

α	specific cake resistance $[m \cdot kg^{-1}]$
α_0	coefficient equal to the specific cake resistance at 1 bar $[m \cdot kg^{-1} \cdot bar^{-n}]$,
β	compressibility index $[-]$
δ	secondary consolidation index $[-]$
γ	modified consolidation coefficient index $[-]$
μ	dynamic viscosity $[Pa \cdot s]$
ν	secondary consolidation coefficient $[-]$
ν_0	coefficient equal to the secondary consolidation index at 1 bar $[bar^{-\delta}]$
ρ	density $[kg \cdot m^{-3}]$
σ	standard deviation
ω	dry mass of solids in the press per filtration surface area $[kg \cdot m^{-2}]$

Indices

0	at the beginning of the operation
atm	atmospheric
av	average in the cake thickness
c	during the consolidation
$cake$	dewatered or in the process of being dewatered mash
$filt$	filtrate
s	solid
tr	at the transition point between the filtration and the consolidation
w	water
∞	at the end of the consolidation, when the equilibrium is reached

1. Introduction

Cassava is estimated as the ninth most considerable crop in the world human diet with 304 million of tons produced in 2019, of which 63% were produced in Africa (Food and Agriculture Organization of the United Nations (2021)). Its production has been increasing for many years, particularly in Africa where it increased by 61% between 2009 and 2019 (Food and Agriculture Organization of the United Nations (2021)). Its transformation is fundamental to extend its shelf-life and reduce its toxicity (Hillocks (2002)).

In Africa, cassava roots are mainly transformed for human consumption, in dry flours, semolina, or fermented pastes (Westby (2002)). During flour production, cassava roots are firstly peeled and washed. Then, depending on the desired product, roots can be fermented, either by immersing entire roots into water, or in bags after grating. The mash obtained is mechanically dewatered, generally by pressing the bags under a piston press, and finally dried. In small processing units, sun drying is often preferred, while it can take a long time (about $27-35\ h$ (Njie and Rumsey (1998))), during which fungus can grow causing mycotoxin production (Westby (2002)). To avoid these problems, to increase and to stabilise the production, artificial dryers are used when it is economically consistent. To limit sun drying time or artificial drying energy consumption, prior mechanical dewatering appears as a crucial step: the more effective this step is, the less energy shall be consumed in the following drying stage.

The three main techniques of mechanical dewatering are: centrifugation, vacuum filtration, and compression. Compression is a relevant technological choice for cassava dewatering in large, medium or small units for many reasons. First, pressing can be performed with a simple and cheap piston press, although centrifugation and vacuum filtration are usually expensive. Moreover, some pressure filters were proved more effective than centrifuges for starch dewatering (Sriroth et al. (1999)).

Data on cassava mechanical dewatering is scarce in literature. Therefore, the present study focused on modelling cassava compression dewatering based on a series of experiments in a filtration-consolidation cell. Cassava from different origins and with different particle size distributions were studied. The objectives were to (i) evaluate the overall performance of the operation and (ii) provide a model for the design of pressing equipment. For this purpose, the proposed model should predict the moisture content of the cake according to the mash initial moisture content and mass, filtration surface area, pressure and time. In the present study, the overall performance of cassava mash compression dewatering was evaluated by monitoring the moisture content of the product in the filtration-consolidation cell over time, at various pressures and for various ratios of pulp mass to filtration surface areas. During the operation, the product undergoes two phenomena, *i.e.* cake filtration and consolidation (Shirato et al. (1970)) . Consolidation begins when the piston reaches the particles, networked enough to form a cake. Robust models, validated on a large variety of products, exist both for filtration (Hermia) and consolidation (*e.g.* Terzaghi, Terzaghi-Voigt, Sivaram and Swamee (1977); Shirato et al. (1979)). For each stage, a model was chosen based on its consistency with the product behaviour and its suitability for applications in engineering (*e.g.* required computing time). Then, both models were combined to describe the whole process. Cake characteristics are defined as pressure-dependent functions, allowing to employ the global model (filtration and consolidation) under various pressures. In the literature, few examples focused on modelling both phenomena (*e.g.* Mihoubi et al. (2003); Grimi et al. (2010)). Moreover, the cake filtration and consolidation properties, as well as the transition point between both phenomena, are generally defined by graphical means (Tarleton and Wakeman (2006)), which is time-consuming and presents repeatability issues due to human

interpretation. To avoid the main limits of this method, *i.e.* the low repeatability and the subjective and time consuming human intervention, a numerical method was proposed and discussed in the present study.

2. Materials and methods

2.1. Cassava mash

Experiments were conducted with three batches of cassava roots: a large batch imported from Costa Rica, noted batch #1, and two smaller batches imported from Costa Rica and Cameroon at different dates, respectively noted batch #2 and #3.

The three batches were manually peeled and rasped to obtain a mash with a defined median particle size. In accordance with the literature data about cassava mash from processing units (Gévaudan (1989); Escobar et al. (2018)), mashes having a d_{50} in an approximate range of $700 - 1000\ \mu m$ were produced. Mash having a d_{50} of $1000\ \mu m$ was obtained with a semi-industrial grater *Gauthier* (France), having the same design as the ones used in cassava processing units. Mash having a d_{50} of $700\ \mu m$ was obtained with a domestic *Magimix cuisine system 4200* (France) kitchen equipment.

To characterise the particle size distribution, a sieving method was adopted. It consists in passing the product through a series of calibrated sieves stacked on top of each other with decreasing mesh sizes. At the end of the procedure, the weight of product retained on each sieve is measured. As cassava mash is very humid ($X = 64.1\%\ w.b.$ here), dry sieving was unsuitable. Thus, a similar protocol based on Da et al. (2013); Escobar et al. (2018) was developed. Cassava mash was sieved with a pile of seven sieves of decreasing mesh sizes (3000, 1000, 710, 425, 212, 106 and 50 μm) under water on a laboratory vibrating sieve machine. Due to the addition of water, the mash retained on each sieve had to be dried afterwards and the amount of dry matter released in the water was evaluated by measuring its dry matter content (method in section 2.2.2). The particle size distributions were based on these dry matters. The amount of released dry matter was neglected in the calculation of the median diameter, as carried out in the literature (Da et al. (2013); Escobar et al. (2018)), while it was considered in the discussion about the product structure in section 3.1.2.

According to the methodology adopted to produce the mash, some cell damage could be observed (Escobar et al. (2021)), which can modify the filtration-consolidation behaviour of the product. Thus, a methodology to estimate a damaged cell ratio was conducted. A specific study about the impact of the conservation method on mash behaviour was also proposed through a preliminary study.

Damaged cell ratio The damaged cell ratio was evaluated following the method proposed by Escobar et al. (2021). Cassava roots are mainly composed of starch (93% dry basis), fibres (2% dry basis) and proteins (3% dry basis) (Aryee et al. (2006)). As in plant tissues, a large part of the starch is located inside the cells, the proportion of cell wall

breakdowns was considered equivalent to the proportion of extracellular starch. The quantity of starch released after rinsing the mash was considered equivalent to the quantity of extracellular starch. In addition, the particle size of cassava starch ranges from 3 to 32 μm (Defloor et al. (1998)). Therefore, mashes were rinsed above a 50 μm mesh size sieve, assuming that the dry matter released was mainly composed of starch. The dry matter content of the rinsing water and the initial mash were finally measured, following the method presented in section 2.2.2. Assuming that the initial mash is composed of 93% dry basis of starch (Aryee et al. (2006)), the proportion of released starch, considered equal to the proportion of damaged cell was calculated.

This procedure allowed establishing that the *Magimix cuisine system 4200* cooking equipment broke 61% of the cell walls, while 64% were broken by the *Gauthier* grater. These proportions are close to the one measured by Escobar et al. (2018) on cassava rasped in *Gari* processing unit, *i.e.* around 65%.

Conservation method As cassava has a short shelf-life, to ensure a good reproducibility of the trials, a conservation technique of the mash had to be chosen. Hence, in a preliminary study, the effects of deep-freezing (at $-25°C$) were evaluated both on the integrity of mash cells and the behaviour of the mash under filtration and consolidation.

The impact of deep-freezing on the integrity of mash cells was evaluated following the method proposed by Escobar et al. (2021) and explained above. The mass difference on released starches, between fresh and frozen mashes grated with *Gauthier* and *Magimix* devices was smaller than 2%. Therefore, freezing procedure on cassava mash seemed to not significantly damage cellular walls.

The impact of deep freezing on the behaviour of the mash under filtration and consolidation was evaluated by comparing compression dewatering experiments in the same conditions (15 *bar*, 200 *g* of mash at the initial time), on both fresh and deep-frozen mashes from the batch #2. As the resulting kinetics were similar (RMSE on the filtrate mass = 2%), the impact of deep-freezing on cassava mash behaviour under filtration and consolidation was considered to be negligible. Therefore, kinetics on deep-frozen mash could be used to fit the model and analyse the dewatering performance.

Table 1 summarises the preparation, conservation and use of the three batches.

2.2. Compression dewatering experiments

2.2.1. Experimental procedure

The filtration-consolidation cell, presented in figure 1, was designed and manufactured at Cirad Laboratories (Qualisud team, Montpellier, France). The cell is a stainless-steel cylinder of 50 *mm* in diameter and 230 *mm* in height. It was closed at the bottom with a valve where a cloth filter collected in a cassava starch factory, having a mesh size of $15-20$ μm, was placed. Pressure applied by the pneumatic piston could be adjusted between 4 and 21 *bar*. A *LabView*

program controlled the pressure applied and recorded, every second, the measurements useful to evaluate the applied pressure (*i.e.* air pressure and strength applied by the piston), and the dewatering kinetics (*i.e.* piston height and filtrate mass).

For trials with deep-frozen mash, the sample was thawed in a bain-marie at 35°C. For trials with fresh mash, the sample was grated within a few hours before the dewatering. The sample thus prepared was inserted in the filtration-consolidation cell. The piston was lowered until touching the mash. The pressure previously entered in the *LabView* program was then applied by the piston on the mash to dewater it. The height of mash in the cell and the mass of filtrate released were measured and recorded during the whole kinetic. When the variation of filtrate mass over time became negligible (*i.e.* less than 0.1 $g \cdot min^{-1}$), the dewatering was stopped by lowering the applied pressure to ambient pressure. The dewatered mash, called filter cake, and the filtrate were weighted. Their dry matter content were measured (see method in section 2.2.2).

The overall performance of the operation and the model calibration were based on the evolution of the product moisture content over time in the filtration-consolidation cell. It was calculated either with the initial mash or the final cake dry matter contents and the filtrate mass. A mass balance on the dry matter of the initial mash, final cake and filtrate allowed to evaluate the validity of a trial. The mass balance on the dry matter of the initial mash, final cake and filtrate was systematically verified.

By comparing several trials with the same pressure, the standard deviation (σ) of the cake moisture content during the whole kinetic was calculated. Therefore, the standard deviation evaluated as a function of the cake moisture content ($\sigma = f(X_{cake})$) was expressed and approximated with a linear function. Each error bar shown on the plots in section 3 has a total height of 2σ.

2.2.2. Dry matter content measurement

For each filtration-consolidation trial, the dry matters of the initial mash, the final cake and the filtrate were measured using different methods. For the cake and the initial mash, the sample was placed on a dry aluminium cup and the ensemble was dried for at least 1 day at 105°C, as recommended by the AOAC (Horwitz and Latimer (2010)). For the filtrate, to avoid measurement errors due to Maillard reactions (Bradley (2010)), the sample was first dried at 45°C under ambient pressure for one day, and next at 70°C under vacuum for another day.

2.3. Modelling of compression dewatering

2.3.1. Modelling strategy

In the filtration-consolidation cell, as mentioned in section 1, the mash undergoes two successive phenomena, *i.e.* filtration and consolidation (Tarleton and Wakeman (2006); Shirato et al. (1970)). Robust models exist for each phenomenon.

Filtration model Depending on filtration conditions, various filtration models can be used. During the compression dewatering of cassava mash, the particles of this highly charged suspension, accumulated on a support (filter), form a porous cake. A cake filtration model can thus be considered (Ripperger et al. (2009)).

Darcy's law was applied and integrated with the following hypothesis to obtain the Hermia model of cake filtration (equation 1, Leclerc (1997)). All the mash solid matter was assumed to be retained on the cloth filter, and thus (i) the mass of deposited cake was assumed to be proportional to filtrate volume and (ii) the filtrate solid matter content was neglected. Therefore, the filtrate viscosity, considered constant, was assimilated to that of water. The pressure applied and the filtration surface area were both considered constant. The filtration phenomenon was assumed to be ideal, *i.e.* cake particles were considered as perfectly rigid and not compactable. Cake structure was therefore considered homogeneous both in space and in time.

$$\frac{t}{Vol_{filt}} = \frac{\mu_{filt} \cdot \alpha_{av} \cdot W}{2 \cdot A^2 \cdot (P - P_{atm})} \cdot Vol_{filt} + \frac{\mu_{filt} \cdot R_s}{A \cdot (P - P_{atm})} \tag{1}$$

With α_{av} the specific cake resistance $[m \cdot kg^{-1}]$, W the mass of deposited dry cake per unit of filtrate volume $[kg \cdot m^{-3}]$, P the pressure applied $[Pa]$, P_{atm} the atmospheric pressure $[Pa]$, R_s the cloth filter resistance $[m^{-1}]$, A the filtration surface area $[m^2]$, Vol_{filt} the filtrate volume $[m^3]$ and t the time $[sec]$, μ_{filt} the filtrate dynamic viscosity $[Pa \cdot s]$.

As a highly charged suspension was filtered, a filter cake should be formed quickly on the support. Thus, the cloth filter resistance was considered negligible (*i.e.* $R_s = 0$) compared to the cake resistance. For some products, considered as compressible, the specific cake resistance is pressure-dependent. In this case, its specific resistance is then described by a power function (equation 2, Tarleton and Wakeman (2006)), involving a compressibility index, n, and a coefficient, α_0, whose value is equal to the specific cake resistance under atmospheric pressure.

$$\alpha_{av} = \alpha_0 \cdot (1 - n) \cdot P^n \tag{2}$$

With α_0 a coefficient $[m \cdot kg^{-1} \cdot bar^{-n}]$, n the compressibility index $[-]$, P the pressure applied $[bar]$

Consolidation model When the piston reaches the cake, filtration ends and consolidation begins. The water is then expelled from the pores, through the reduction of the porosity and the thickness of the cake. Consolidation can generally be divided into two successive stages, named the primary and the secondary consolidation.

The primary consolidation is characterised by cake porosity variation depending only on the local pressure applied. It ends locally when the hydraulic pressure becomes equal to the atmospheric pressure, all the applied pressure being supported by the solid matrix.

Primary consolidation can be described by a diffusive model based on Terzaghi's theory developed for soil engineering and then applied to other fields (Kamst (1995); Venter et al. (2007)). Terzaghi considered (i) consolidation as unidimensional, *i.e.* with only vertical constraints, deformations and water flow and (ii) the consolidation coefficient as constant both in space and in time to simplify the calculation. This model was applied to filter cakes, considered as having an heterogeneous structure at the beginning of the consolidation (Shirato et al. (1986)). Indeed, during filtration, the layers of the cake close to the filter medium have generally started to be slightly compressed, resulting in a vertical gradient of solid concentration (Leclerc and Rebouillat (1985)). To take into account this heterogeneity, Shirato et al. (1980, 1986) assumed that the initial distribution of hydraulic pressure in a filter cake was the solution of the consolidation model, at the initial time, solved using a Laplace transform: monotone, increasing from the top to the bottom of the cake, and described by a sinusoidal function on a half period.

Considering this initial condition, Shirato et al. (1986) presented an analytical solution of this primary consolidation model for filter cake (equation 3). Details of these models are available in the literature (*e.g.* Shirato et al. (1986); Kamst (1995)).

$$U_c = \frac{L_{tr} - L}{L_{tr} - L_\infty} = 1 - exp\left(-\frac{\pi^2 \cdot T_c}{4}\right) \tag{3}$$

$$T_c = \frac{i^2 \cdot C_e \cdot t_c}{V_{s_0}^2} \tag{4}$$

With U_c the consolidation ratio $[-]$, L_{tr}, L, L_∞ the cake thickness $[m]$, respectively at the beginning of the consolidation, at the time t_c $[s]$ and at the end of the consolidation, T_c the dimensionless consolidation time $[-]$, C_e the modified consolidation coefficient $[m^2 \cdot s^{-1}]$, i the number of drainage surface $[-]$ ($i = 1$ if there is one drainage surface, *i.e.* one filter media, and $i = 2$ if there is one filter on the top and one on the bottom of the cake), V_{s_0} the solid volume per filtration surface area at the initial time $[m^3 \cdot m^{-2}]$.

The secondary consolidation is characterised by cake porosity variation due to the creep of solids (Sivaram and Swamee (1977); Shirato et al. (1974); Leclerc and Rebouillat (1985)). The kinetics of this phenomenon depends mainly

on the plastic characteristics of the solid (Shirato et al. (1970)). Consolidation ends at the equilibrium point, at which the pressure in the cake is uniform and the filtrate is no more expelled.

To take into account both consolidation stages, Shirato et al. (1979), building on the work from Sivaram and Swamee (1977), proposed the semi-empirical model presented in equation 5, which is possibly the most widely applicable model. It was developed for cakes having a homogeneous structure at the beginning of the consolidation.

$$U_c = \frac{L_{tr} - L}{L_{tr} - L_\infty} = \frac{\sqrt{\frac{4 \cdot T_c}{\pi}}}{\left[1 + \left(\frac{4 \cdot T_c}{\pi}\right)^{\nu}\right]^{\frac{1}{2 \cdot \nu}}} \tag{5}$$

With ν the secondary consolidation coefficient $[-]$

Intrinsic characteristics of the product representing its behaviour in consolidation are used in these models. The modified consolidation coefficient C_e reflects the cake compressibility during the consolidation phase. The secondary consolidation coefficient ν indicates the extent of the secondary consolidation phase. A secondary consolidation occurs usually for products having a ν lower than 2.8 (Shirato et al. (1979)). Moreover, to use Shirato et al. (1979, 1986) models in a filtration-consolidation operation, the length of the cake at the transition time, *i.e.* at the end of the filtration, and at the beginning of the consolidation, are needed. These lengths can be calculated from the volume fraction of solids in cake respectively at the transition time ($C_{av_{tr}}$) and at the equilibrium (C_{av_∞}), which are intrinsic characteristics of the product (Tarleton and Wakeman (2006)). As the specific cake resistance in filtration, according to Tarleton and Wakeman (2006), these four characteristics can be expressed as power functions of the pressure applied P by an equation having the form of the equation 6. Specific correlations of each pressure-dependent properties are presented in table 2.

$$Y = Y_0 \cdot P^{Y_1} \tag{6}$$

With Y one of the product characteristics in consolidation (*i.e.* $C_{av_{tr}}$, C_e, C_{av_∞}, ν), Y_0 a coefficient equal to the product characteristic when $P = 1$, Y_1 a parameter and P the pressure applied.

2.3.2. Data processing

For each trial, the characteristics of the product in filtration and consolidation (*i.e.* α_{av}, $C_{av_{tr}}$, C_e, C_{av_∞}, ν) were identified using a numerical method. A graphical method is usually employed when both filtration and consolidation are considered (Tarleton and Wakeman (2006)), requiring a human intervention. To avoid -subjective- human interventions, in particular for parameters as critical as the transition point between both phenomena, and improve the

robustness and the reliability of the procedure, we proposed to use a mathematical, systematic, curve fitting approach. Filtration and consolidation models presented in the previous section were implemented in Python 3.8 language using the constants and properties defined in table 3. The curve fitting method from the Scipy library, based on the Levenberg-Marquardt algorithm, was used to determine the coefficients best suiting the experimental data. It took less than 10 seconds to fit 10 trials on a DELL Latitude 5500 Intel(R) Core(TM) i7-8665U CPU @ 1.90GHz with 16 GB RAM with Windows 10 PRO 64 bits operating systems.

The characteristics of the product identified on a selected subset of experiments, noted *learning set*, were then expressed as a function of the pressure applied P. The selected experiments were kinetics for which (i) identified coefficients had a reasonable confidence interval and (ii) the volume fraction of solids in cake at the end of consolidation, C_{av_∞}, identified numerically, and the mass fraction of water in the cake at the end of consolidation, X_{cake_∞}, measured experimentally, had similar trend when plotted against pressure. The subset of experiments not selected was noted *training set* and used for validation purpose. Finally, the global model, with the pressure-dependent properties, was compared to all data from *learning* and *training sets*.

3. Results and discussion

3.1. Overall performance

3.1.1. Experimental results

The present study was carried out in view of evaluating the performance of cassava pulp dewatering. As the objective was to obtain the cake as dry as possible in a limited time, the performance was discussed in terms of the dewatered cake moisture content and the analysis of the dewatering kinetics.

Dewatered cake moisture content Figure 2 presents the mash moisture content at the end of the consolidation (X_{cake_∞}) as a function of the applied pressure P for cassava mash having different particle size characteristics. The final moisture content of the dewatered cassava mash from the three batches (X_{cake_∞}) strongly depended on the pressure P (Figure 2). X_{cake_∞} decreased quite linearly from 42.5% $w.b.$ at 4 bar, to 34.5% $w.b.$ at 16 bar. At higher pressures, X_{cake_∞} remained stable around 34.5% $w.b.$. Therefore, it can be assumed that it is not possible to extract more water from the mash by increasing the pressure above 16 bar. The cake moisture content measured at 16 bar could be considered as the mash moisture content limit, defined in the literature as being representative of the proportion of bound water (Lee and Hsu (1995); Kopp and Dichtl (2001); Ruiz et al. (2010); Zarate Vilet et al. (2020)). This water is characterized by strong interactions with solids by capillary or adhesive forces (Kopp and Dichtl (2001)) and thus requires thermic process, as drying, to be removed. According to this, 34.5% $w.b.$ seemed to be the minimum moisture content that can be achieved through a mechanical dewatering by filtration-consolidation.

Figure 2 shows that the difference in particle size distribution seemed to have a negligible effect on the X_{cake_∞}. Moreover, as the mashes from the three batches of cassava roots had similar X_{cake_∞} at a same pressure (Table 5), the influence of the variability of raw material was assumed to be negligible.

Kinetics analysis The operating conditions had a strong influence on the dewatering kinetics. An increase of the applied pressure led to a faster dehydration and a larger quantity of filtrate eliminated (Figure 3a). As an example, at 4 bar, for a ratio between the mass of solids and the filtration surface area (ω_0) of 15 $kg\ dry\ matter \cdot m^{-2}$, the equilibrium ($X_{cake_\infty} = 39.0\%\ w.b.$) was almost reached in 1500 s whereas at 21 bar, only 500 s were necessary to reach it ($X_{cake_\infty} = 33.0\%\ w.b.$). Nevertheless, at both pressures, filtrate was still flowing after 6 h. Moreover, an increase in the ratio between the mass of solids and the filtration surface area (ω_0), had also a significant impact on the dewatering time (Figure 3b). At 6 bar, the equilibrium was almost reached in 1500 s for $\omega_0 = 15.0\ kg\ dry\ matter \cdot m^{-2}$, whereas it was reached in 700 s for $\omega_0 = 7.5\ kg\ dry\ matter \cdot m^{-2}$. Actually, twice as much filtrate was extracted in the first case as in the second on the same filtration surface, taking twice as long.

The impact of cassava mash quality, *i.e.* particle size distribution and roots origin, was less remarkable. Actually, no difference between the kinetics of the mash having a d_{50} of 700 μm or 1000 μm could be highlighted. Furthermore, the experimental kinetics on the three batches looked similar. No significant effect of the roots origin on the kinetics could be highlighted.

If the kinetic results are more rigorously analysed in the Modelling part (3.2), the role of cassava mash quality, and specifically of the particle size distribution, is described in the following part.

3.1.2. Discussion

Particle size distribution of cassava mashes rasped by both devices used in the present study were quite similar when the amount of starch, *i.e.* particles finer than the last sieve (50 μm mesh size), was taken into account (Figure 4). They were bimodal, with a high peak of particles having a diameter smaller than 50 μm, called starch peak, and a class of particles between 200 and 3000 μm. As presented in figure 4 and confirmed by their close proportion of ruptured cell walls (section 2.1), both mashes had almost the same proportion of fine particles, *i.e.* 54 and 62%. However, both the difference between their median diameter calculated excluding the starch peak, *i.e.* 700 and 1000 μm, and the figure 4, show the discrepancy in the distribution of their coarser particles (between 200 and 3000 μm). As dewatering kinetics on both mashes were similar (section 3.1.1), the difference in the distribution of coarser particles may have a negligible effect on their behaviour in filtration-consolidation. However, as polydispersion is known to have an important influence on the behaviour of the product in filtration (Li et al. (2021)), a suspension containing only starch may behave differently. Indeed, cassava starch ($X_0 = 64\%\ w.b.$) compressed at 16 bar, reached a moisture

content of 34% *w.b.* in 90 *sec* (Sriroth et al. (1999)), while cassava mash compressed at 16 *bar*, with a ratio between the mass of dry matter and the filtration surface area (ω) 1.5 times lower, only reached a moisture content around 50% *w.b.* in the same time. In addition, starch moisture content limit is around 35% *w.b.* at 16 *bar* (Sriroth et al. (1999); Salmela (2006)). Therefore, the presence of particles coarser than starch in cassava mash significantly slowed down the dewatering of the product, when compared to pure starch behaviour, while it seemed to have a negligible effect on its moisture content limit. A finer fragmentation may thus not influence cassava mash moisture content limit.

Knowing better the cassava mash structure, the influence of its origin in terms of processing unit on its behaviour in compression dewatering can be discussed. Excluding the starch peak, as carried out in the literature, the median diameters of cassava mashes collected in various processing units, reported by Gévaudan (1989); Escobar et al. (2018), were almost in between the ones of the mashes used in the present study (section 2.1). In addition, Escobar et al. (2021) estimated a proportion of broken cells of cassava mash collected in other processing units close to the one estimated on our mashes (section 2.1). Therefore, as cassava mashes collected in various processing units and the ones used in the present study may have similar proportions of fine particles and a bimodal particle size distribution, their behaviours may be similar in compression dewatering, represented by the same model.

3.2. Modelling

For the consolidation stage, the theoretical model representing only the primary consolidation stage (Shirato et al. (1986), equation 3), and the semi-empirical one representing both the primary and the secondary consolidation stages (Shirato et al. (1979), equation 5), were compared to the experiments of the three batches. As it can be noticed in figure 5a, the U_c-curve based upon the primary consolidation stage model matched well the experimental data in the first part of the curve. Although, at $T_c > 1$, the model curve deviated, possibly meaning that the secondary consolidation should be considered. On the contrary, the model considering both stages matched better to the experimental curve (Figure 5b). This comparison was done for at least 10 trials and led to the same conclusions. Thus, the Shirato et al. (1979) equation was chosen to represent the consolidation stage.

The accurate prediction of the experimental data by the Shirato et al. (1979) model means that the secondary consolidation cannot be neglected, and that a homogeneous structure of the cake at the initial time can be considered. The relevance of the Shirato et al. (1979) model also demonstrated that the complexity of the cassava matrix (*e.g.* heterogenic water distribution in the matrix, potential cells rupture during the compression (Lanoisellé et al. (1996)) was not an obstacle to such model applicability. However, for coarsely fragmented cassava, *i.e.* containing more intracellular water, and considering the specificities of cellular material, the model from Lanoisellé et al. (1996) could be more appropriate in some cases. Nonetheless, this latter model being much more computationally intensive and

requiring more knowledge about the product, it appears in any case less adapted to the pre-design of equipment than the Shirato et al. (1979) one.

3.2.1. Experimental validation of the simulation model

42 trial kinetics from the learning and training sets were performed using 21 experimental conditions and three batches of roots, as shown in table 5. All kinetics were similar: a quick dynamic decrease followed by a slow quasi-static stabilisation (Figures 3, 6, 7). The global model with the correlation between the characteristics of the product in filtration-consolidation and the pressure, defined in section 3.2.2, was compared to all these experiments in terms of the evolution of the cake moisture content with time. The prediction errors on the final dry matter content and the product moisture content all along the experiments are summarised in table 4. An average discrepancy (RMSE) of 13% was observed globally and only 14% of the trials presented a discrepancy higher than 16%. Moreover, most simulations gave a precise estimate of both the transient and asymptotic behaviours, *i.e.* within the 2σ (experimental uncertainty) range, while only a few were above the 2σ but still within the 4σ range, see figure 6. Focusing on the first hour of the kinetics, as shown on figure 7, it was observed that the simulation model, while close to the experimental data points, displayed some kind of discontinuous transition between filtration and consolidation. Still, the simulations remained very close to experimental data, almost always within the experimental uncertainties. In addition, when looking carefully at the residues (*i.e.* the model-experiment difference), it was observed that they were equally distributed, meaning that there is no systematic under or over-estimation.

Both RMSE and error on the final cake moisture content prediction were similar for the three batches, suggesting a negligible impact of the batch origin, as suggested earlier (Figures 6, 7). This remark should be balanced when looking at the slight difference that can be observed on the transient part of the kinetics of batch #2 with a mass of dry matter per filtration surface area ω_0 of 30 $kg\ dry\ matter \cdot m^{-2}$. This difference could be due either to the mash origin or to the actual ω_0, higher than the one chosen for most of the kinetics (*i.e.* $\omega_0 = 15\ kg\ dry\ matter \cdot m^{-2}$). Still, the model fits quite well all kinetics of the 3 batches.

3.2.2. Product characteristics in filtration and consolidation

The five product characteristics in filtration and consolidation were identified (*i.e.* α_{av}, $C_{av_{tr}}$, C_e, C_{av_∞}, ν) and expressed as functions of the pressure P (Table 2). They were used in the global model compared to the dewatering kinetics in section 3.2.1. As stated in section 2.3.2, 25 experiments from the three batches, noted learning set, among 41 in total, were selected to define the correlation between these characteristics and the pressure (Figure 8).

The weak pressure-dependency of the volume fraction of solids in the mash at the end of the filtration stage $C_{av_{tr}}$ and of the specific cake resistance α_{av} (Figure 8) was considered as negligible to limit the number of parameters

of the model. Therefore, their average values were considered for the model, namely $C_{av_{tr}} = 0.45 \pm 0.046$, $\alpha_{av} = 6.5 \cdot 10^{11} \pm 2.2 \cdot 10^{11}\ m \cdot kg^{-1}$. As the average RMSE between the model and the experimental kinetics was below 13% (see section 3.2.1), these assumptions were considered acceptable. The weak pressure-dependency of the specific cake resistance α_{av} is interesting for industrial operation in the sense that an increase in pressure will accelerate the dewatering kinetics, and thus allow a faster attainment of $C_{av_{tr}}$.

For the characteristics in consolidation, on one hand, no significant trend could be highlighted between the consolidation coefficient ν and the pressure P. Its average value, namely $\nu = 0.98 \pm 1.44$, was then considered. As $\nu < 2.8$, both primary and secondary consolidation occurred (see section 3.2.2). On the other hand, the modified consolidation coefficient C_e, representing the cake compressibility, increased with the pressure, slightly slowing down the consolidation. Furthermore, the volume fraction of solids in the mash at the end of the consolidation C_{av_∞} and the final cake moisture content X_{cake_∞}, representing the same physical variable, had consistent trends when plotted against the pressure (Figures 2, 8). Therefore, increasing pressure up to 16 *bar* would slightly slow down the consolidation and significantly decrease the dewatered mash moisture content. Above 16 *bar*, as the limit dryness is reached (section 3.1.1), a pressure increase during the consolidation stage would not further reduce the final moisture content and would only slow down the dewatering. The equations presented in table 2 were fitted to C_{av_∞} $[-]$ and C_e $[m^2 \cdot s^{-1}]$, with the pressure P $[bar]$, and resulted as $C_{av_\infty} = 0.45 \cdot P^{0.094}$ and $C_e = 6.6 \cdot 10^{-8} \cdot P^{0.84}$. Finally, the volume fraction of solids at the end of the filtration ($C_{av_{tr}}$) and at the end of the consolidation (C_{av_∞}) indicate that most of the water was extracted during the filtration stage.

In view of the cake characteristics identified here, the models used and the performance analysis in section 3.2.2, general guidelines for improving the operation can be identified. Increasing the pressure during the filtration stage or increasing the filtration surface area would significantly reduce the operation time. Moreover, if compression dewatering is followed by drying, to minimise the energy requirement, it could be recommended to work at 16 *bar* to achieve the minimum moisture content. Nonetheless, depending on the context, this may not be the techno-economic optimum since the cost of the equipment is likely to be strongly related to the pressure level.

In addition, it could be stated that between the two particle sizes, there were no remarkable differences on the coefficients fitted, which is consistent with the experimental kinetics analysis (section 3.1.1). Therefore, the identified coefficients are valid for mash having the particle size distribution measured in processing units (Gévaudan (1989); Escobar et al. (2018)). This may be due to the small difference in particle sizes, as explained in section 3.1.2. Finally, the coefficient values presented above are valid for cassava mash having a d_{50} in a $700 - 1000\ \mu m$ range. The origin of the raw material did not either have an effect on the coefficients, which characterise the product properties. In this modelling approach, this raw material variability has therefore a non-significant impact on the product behaviour.

3.2.3. *Evaluation of the physical consistence of the fitting method*

The product characteristics are usually defined using a graphical method when both filtration and consolidation phenomena are considered (Tarleton and Wakeman (2006)). Various plots allowed to identify, successively, (i) the transition time (*i.e.* the time at which filtration ends and consolidation begins), (ii) the specific cake resistance α_{av}, (iii) the modified consolidation coefficient C_e. The volume fraction of solids in the mash at the end of the filtration stage $C_{av_{tr}}$ and at the end of the consolidation stage C_{av_∞} are calculated respectively with the mash moisture content at the transition time and at the end of the consolidation. The secondary consolidation coefficient ν was then identified by minimising the RMSE. The identification of the characteristics and particularly the transition point was weakly repeatable. Nevertheless, it ensured that the identified coefficients had a physical meaning.

The identification method proposed in the present study, based on curve fitting, can also be considered as physically consistent. Actually, the transition time calculated with the identified coefficients was placed at the point at which a change in behaviour was visible on the graphs used in the graphical method (Tarleton and Wakeman (2006)). Moreover, volume fraction of solids in the cake identified were physically consistent. The C_{av_∞} identified was consistent, although slightly higher, with the C_{av_∞} computed directly from experimental measurements. In addition, the identified coefficient equal to the volume fraction of solids at the end of a consolidation at atmospheric pressure was almost equal to the volume fraction of solids identified at the transition point (both about 0.45), himself significantly higher than the one measured before dewatering on the rasped mash (about 0.28), *i.e.* $C_{0_\infty} \simeq C_{av_{tr}} > C_0$. Therefore, at atmospheric pressure, cassava mash would be dewatered by filtration until reaching $C_{av_{tr}}$ and the consolidation phenomena would be negligible.

4. Conclusion

Cassava roots from three origins, grated at two different particle sizes, were dewatered in a filtration-consolidation cell between 4 and 21 *bar*. The final moisture content of the product decreased linearly with increasing pressure from 4 to 16 *bar*, where the moisture content limit was reached at 34.5% wet basis. No significant effect of particle size distribution or roots origin on the dewatering performance could be highlighted. The dewatering speed significantly increased with increasing pressure, a behaviour that is typical of incompressible cake filtration. This was further analysed through modelling.

By comparing the experimentally measured dewatering kinetics to physical and semi-empirical models available in the literature, the mechanisms involved were identified. The product undergoes two successive phenomena : a cake filtration stage, described by Hermia model, followed by a consolidation stage, described by Shirato et al. (1979) model. These models were combined in a global model, fitted on each filtration-consolidation experiment with a

robust and repeatable numerical procedure, allowing fast data processing. The intrinsic characteristics of the product thus identified were then expressed as a function of pressure. The global model using these pressure-dependent characteristics, was validated for cassava mash having a d_{50} in a $700 - 1000\ \mu m$ range, dewatered in a $4 - 21\ bar$ pressure range. The input to the model were the residence time, the filtration surface area, the applied pressure, the mass and initial moisture content of the cassava mash and the output was the dewatering kinetic. On the 42 filtration-consolidation experiments, it predicted the moisture content of the cassava mash with a mean discrepancy (RMSE) of 13%.

The proposed model constitutes a basis for the design of larger-scale dewatering equipment. The main perspectives of the present study are the evaluation of the validity of the model on a larger scale and the development of a techno-economic model of the equipment. Finally, by coupling this model to a dryer model, engineers may define the optimal design of the combination of these two stages according to their constraints, notably processing time, operating and investment costs.

Acknowledgements

We would like to thank Patrice Thaunay, Eric Martin, Jean-Paul Fleuriot and Charlène Lancement for the design and manufacture of the filtration-consolidation cell. We would like to thank Dr. Michèle Delalonde for the discussion about the product structure. We also gratefully acknowledge Dr. Dominique Dufour for facilitating this work as project coordinator.

Funding

The research to prepare the present study was undertaken as part of, and funded by, the CGIAR Research Program on Roots, Tubers and Bananas (RTB) and supported by CGIAR Trust Fund contributors (https://www.cgiar.org/funders/) and French Agricultural Research Centre for International Development (Cirad), Montpellier, France.

References

Aryee, F., Oduro, I., Ellis, W., and Afuakwa, J. (2006). The physicochemical properties of flour samples from the roots of 31 varieties of cassava. *Food Control*, 17(11):916–922.

Bradley, R. L. (2010). Moisture and total solids analysis. In *Food analysis*, pages 85–104. Springer.

Da, G., Dufour, D., Giraldo, A., Moreno, M., Tran, T., Velez, G., Sanchez, T., Le-Thanh, M., Marouze, C., and Marechal, P.-A. (2013). Cottage level cassava starch processing systems in Colombia and Vietnam. *Food and Bioprocess Technology*, 6(8):2213–2222.

Defloor, I., Dehing, I., and Delcour, J. A. (1998). Physico-chemical properties of cassava starch. *Starch - Stärke*, 50(2-3):58–64.

Escobar, A., Dahdouh, L., Rondet, E., Ricci, J., Dufour, D., Tran, T., Cuq, B., and Delalonde, M. (2018). Development of a Novel Integrated Approach to Monitor Processing of Cassava Roots into Gari: Macroscopic and Microscopic Scales. *Food and Bioprocess Technology*, 11(7):1370–1380.

Escobar, A., Rondet, E., Dahdouh, L., Ricci, J., Akissoé, N., Dufour, D., Tran, T., Cuq, B., and Delalonde, M. (2021). Identification of critical versus robust processing unit operations determining the physical and biochemical properties of cassava-based semolina (gari). *International Journal of Food Science & Technology*, 56(3):1311–1321.

Food and Agriculture Organization of the United Nations (2021). FAOSTAT statistical database. Online; accessed 9 December 2021.

Grimi, N., Vorobiev, E., Lebovka, N., and Vaxelaire, J. (2010). Solid–liquid expression from denaturated plant tissue: Filtration–consolidation behaviour. *Journal of Food Engineering*, 96(1):29–36.

Gévaudan, A. (1989). *Etude du séchage par contact de milieux granulaires agités*. PhD thesis, Institut National des Sciences Appliquees de Lyon.

Hillocks, R. J. (2002). *Cassava in Africa*. CABI, Wallingford.

Horwitz, W. and Latimer, G. (2010). *Official methods of analysis of AOAC International. Volume I, agricultural chemicals, contaminants, drugs*. Gaithersburg (Maryland): AOAC International, 1997.

Kamst, G. F. (1995). *Filtration and expression of palm oil slurries as a part of the dry fractionation process*. PhD thesis, Technische Universiteit Delft, Netherlands.

Kopp, J. and Dichtl, N. (2001). Influence of the free water content on the dewaterability of sewage sludges. *Water Science and Technology*, 44(10):177–183.

Lanoisellé, J.-L., Vorobyov, E. I., Bouvier, J.-M., and Pair, G. (1996). Modeling of solid/liquid expression for cellular materials. *AIChE journal*, 42(7):2057–2068.

Leclerc, D. (1997). Filtration sur support aspects théoriques. *Techniques de l'ingénieur Opérations unitaires. Génie de la réaction chimique.*, base documentaire : TIP452WEB.(ref. article : j3501).

Leclerc, D. and Rebouillat, S. (1985). Dewatering by compression. In *Mathematical models and design methods in solid-liquid separation*, pages 356–391. Springer.

Lee, D. and Hsu, Y. (1995). Measurement of bound water in sludges: a comparative study. *Water Environment Research*, 67(3):310–317.

Li, B., Zhang, H., Saranteas, K., and Henson, M. A. (2021). A rigid body dynamics model to predict the combined effects of particle size and shape on pressure filtration. *Separation and Purification Technology*, 278:119462.

Mihoubi, D., Vaxelaire, J., Zagrouba, F., and Bellagi, A. (2003). Mechanical dewatering of suspension. *Desalination*, 158(1-3):259–265.

Njie, D. N. and Rumsey, T. R. (1998). Experimental study of cassava sun drying. *Drying Technology*, 16(1-2):163–180.

Ripperger, S., Gösele, W., and Alt, C. (2009). Filtration, 1. Fundamentals. In Wiley-VCH Verlag GmbH & Co. KGaA, editor, *Ullmann's Encyclopedia of Industrial Chemistry*, volume 14, pages 677–709. Wiley-VCH Verlag GmbH & Co. KGaA, Weinheim, Germany.

Ruiz, T., Kaosol, T., and Wisniewski, C. (2010). Dewatering of urban residual sludges: Filterability and hydro-textural characteristics of conditioned sludge. *Separation and Purification Technology*, 72(3):275–281.

Salmela, N. (2006). *Washing and dewatering of different starches in pressure filters*. PhD thesis, Lappeenrannan Teknillinen Yliopisto, Lappeenranta. OCLC: 255795673.

Shirato, M., Murase, T., and Atsumi, K. (1980). Simplified computational method for constant pressure expression of filter cakes. *Journal of Chemical Engineering of Japan*, 13(5):397–401.

Shirato, M., Murase, T., Atsumi, K., Aragaki, T., and Noguchi, T. (1979). Industrial expression equation for semi-solid materials of solid-liquid mixture under constant pressure. *Journal of Chemical Engineering of Japan*, 12(1):51–55.

Shirato, M., Murase, T., Iritani, E., and Nakatsuka, S. (1986). Analysis of consolidation process in filter cake dewatering by use of difficult-to-filter slurries. *Journal of chemical engineering of Japan*, 19(6):587–592.

Shirato, M., Murase, T., Negawa, M., and Senda, T. (1970). Fundamental studies of expression under variable pressure. *Journal of Chemical Engineering of Japan*, 3(1):105–112.

Shirato, M., Murase, T., Tokunaga, A., and Yamada, O. (1974). Calculations of consolidation period in expression operations. *Journal of Chemical Engineering of Japan*, 7(3):229–231.

Sivaram, B. and Swamee, P. (1977). A computational method for consolidation-coefficient. *Soils and Foundations*, 17(2):48–52. Publisher: The Japanese Geotechnical Society.

Sriroth, K., Walapatit, S., Chollakup, R., Chotineeranat, S., Piyachomkwan, K., and Oates, C. G. (1999). An improved dewatering performance in cassava starch process by a pressure filter. *Starch-Stärke*, 51(11-12):383–388.

Tarleton, S. and Wakeman, R. (2006). *Solid/Liquid Separation: Equipment Selection and Process Design*. Elsevier.

Venter, M., Schouten, N., Hink, R., Kuipers, N., and de Haan, A. (2007). Expression of cocoa butter from cocoa nibs. *Separation and Purification Technology*, 55(2):256–264.

Westby, A. (2002). Cassava utilization, storage and small-scale processing. In Hillocks (2002), pages 281–300.

Zarate Vilet, N., Gué, E., Servent, A., Delalonde, M., and Wisniewski, C. (2020). Filtration-compression step as downstream process for flavonoids extraction from citrus peels: Performances and flavonoids dispersion state in the filtrate. *Food and Bioproducts Processing*, 120:104–113.

List of Figures

1 Schematics of the filtration-consolidation lab scale pilot. 21
2 Mash moisture content at the end of the consolidation (X_{cake_∞}) as a function of the applied pressure P. 22
3 Effect of the operating conditions on the dewatering kinetics. 23
4 Particle size distribution of rasped cassava mash before dewatering. 24
5 Comparison of an experimental data set with selected consolidation models. Only the consolidation stage is plotted: $T_c = 0$ at the transition time between the filtration and the consolidation stages. 25
6 Compression dewatering kinetics. 26
7 Focus on the first part of cassava mash dewatering kinetics. 27
8 Characteristics of cassava mash in filtration and consolidation: relation to pressure. 28

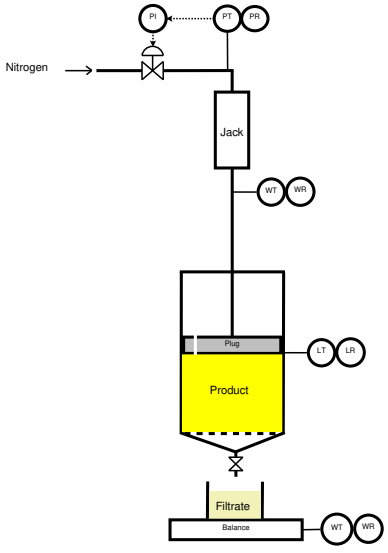

(a) Instrumentation diagram. With LR the length recorder; PI the pressure indicator; PR the pressure recorder; PT the pressure transmitter; WR the strength recorder.

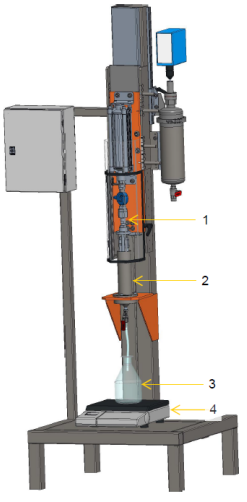

(b) 3D image. With (1) the pneumatic piston; (2) the cell were the product is filtered and consolidate; (3) the filtrate vessel; (4) the filtrate balance.

Figure 1: Schematics of the filtration-consolidation lab scale pilot.

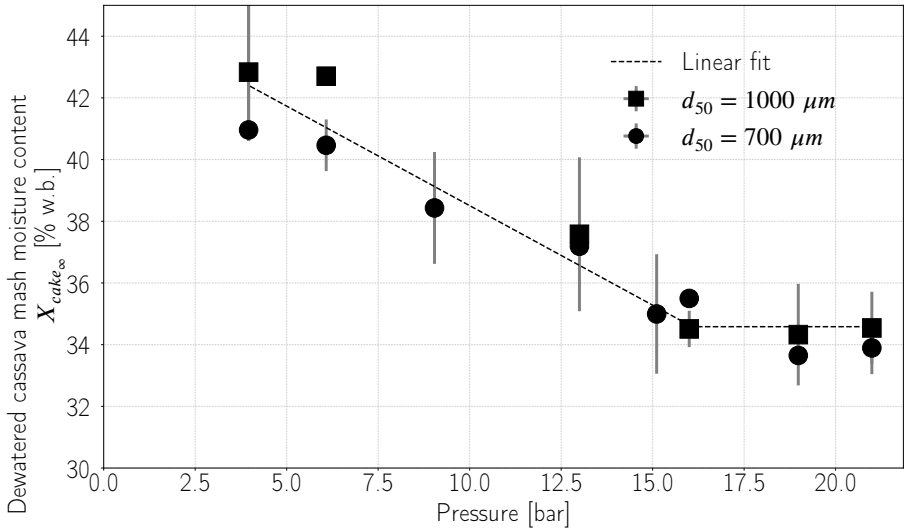

Figure 2: Mash moisture content at the end of the consolidation (X_{cake_∞}) as a function of the applied pressure P.

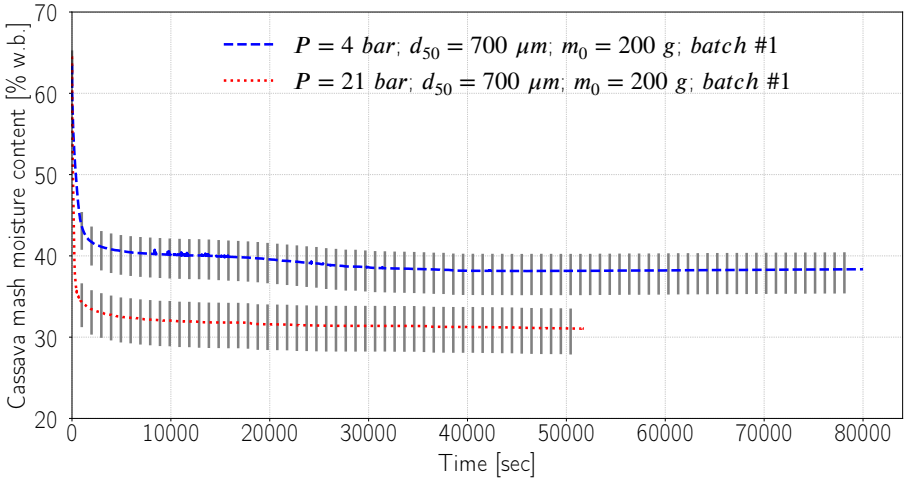

(a) Effect of the pressure on the dewatering kinetics.

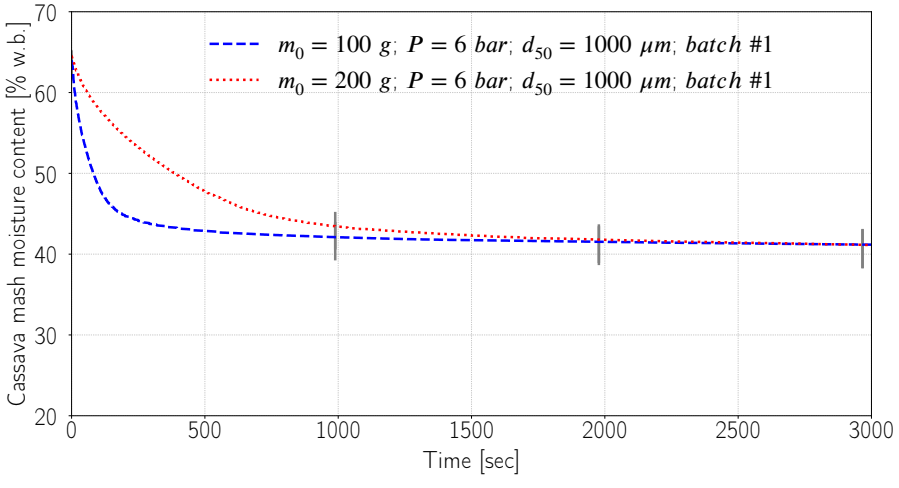

(b) Effect of the ratio between the mass of solids and the filtration surface area. For a better readability, the plot focuses on the first part of the kinetics.

Figure 3: Effect of the operating conditions on the dewatering kinetics.

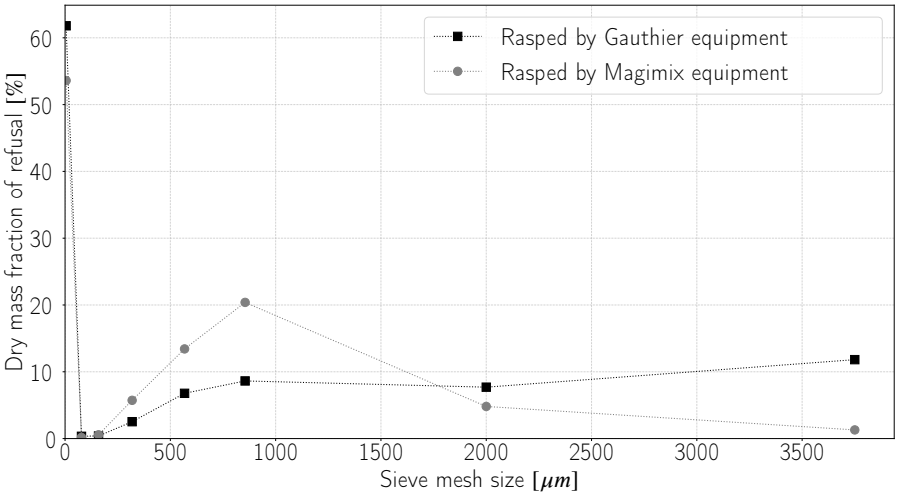

Figure 4: Particle size distribution of rasped cassava mash before dewatering.

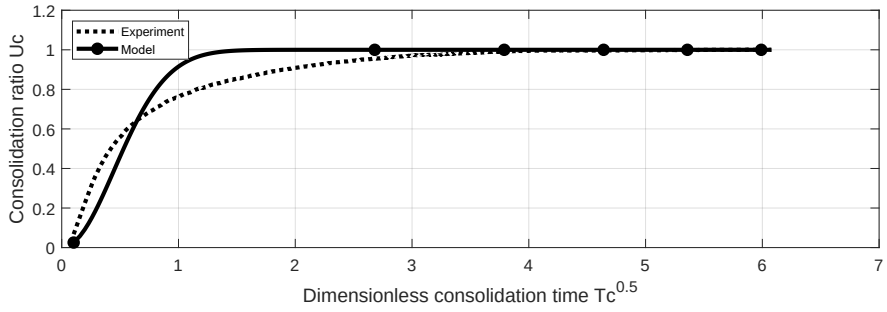

(a) Shirato et al. (1986) theoretical model based on Terzaghi's theory, considering only the primary consolidation.

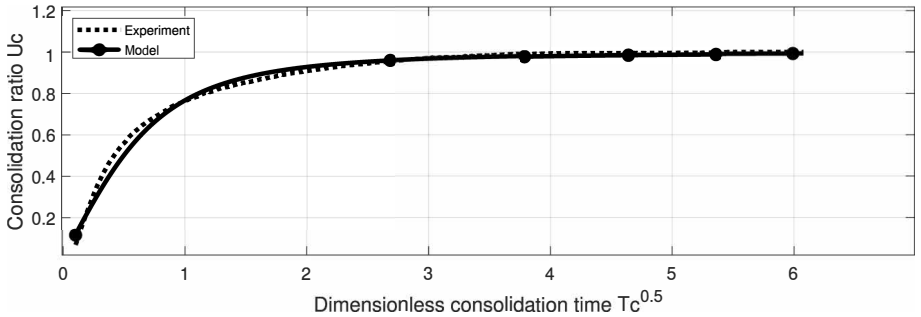

(b) Shirato et al. (1979) semi-empirical model, considering both primary and secondary consolidation.

Figure 5: Comparison of an experimental data set with selected consolidation models. Only the consolidation stage is plotted: $T_c = 0$ at the transition time between the filtration and the consolidation stages.

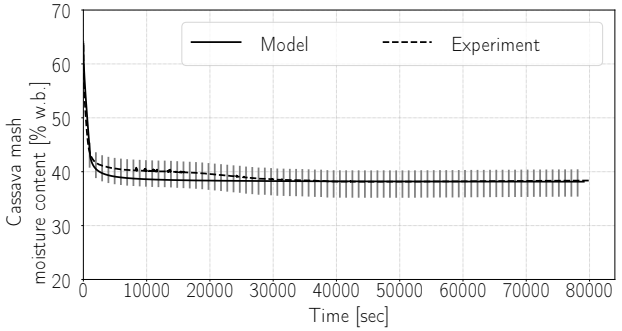

(a) $P = 4.0\ bar$, $m_0 = 200\ g$, $d_{50} = 700\ \mu m$, $batch\ \#1$

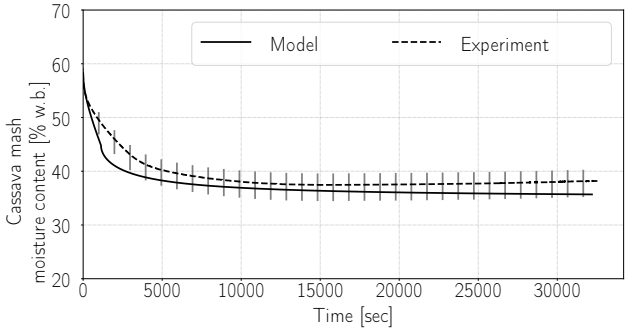

(b) $P = 9.0\ bar$, $m_0 = 400\ g$, $d_{50} = 700\ \mu m$, $batch\ \#2$

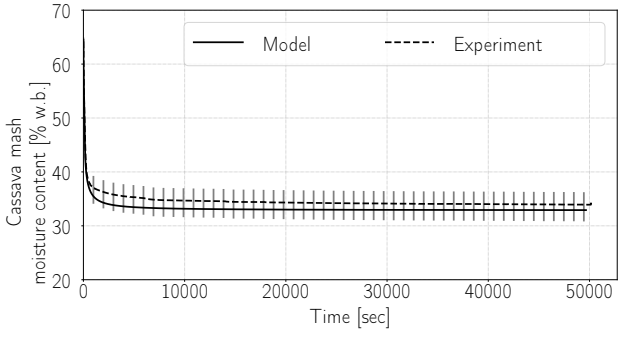

(c) $P = 19\ bar$, $m_0 = 200\ g$, $d_{50} = 1000\ \mu m$, $batch\ \#1$

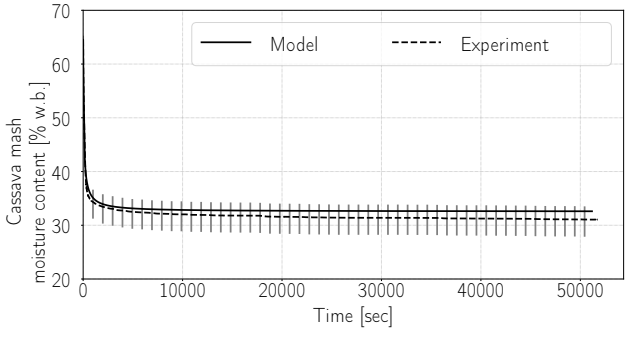

(d) $P = 21\ bar$, $m_0 = 200\ g$, $d_{50} = 700\ \mu m$, $batch\ \#1$

Figure 6: Compression dewatering kinetics.

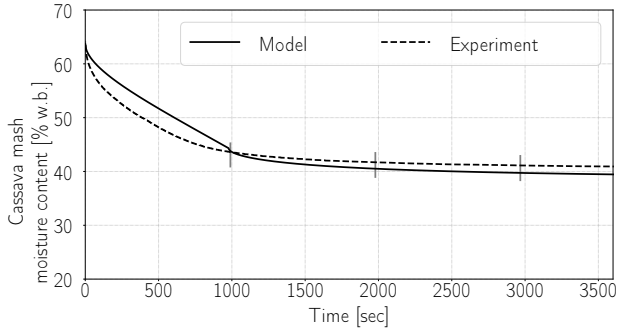

(a) $P = 4.0\ bar$, $m_0 = 200\ g$, $d_{50} = 700\ \mu m$, $batch\ \#1$

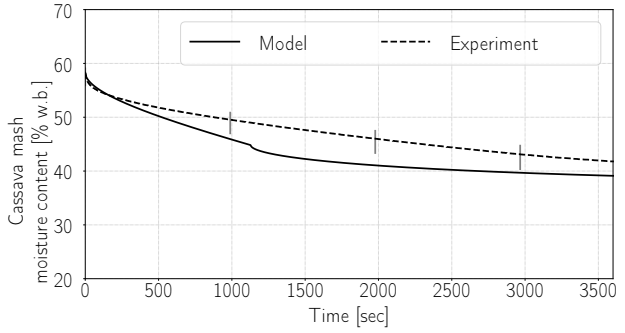

(b) $P = 9.0\ bar$, $m_0 = 400\ g$, $d_{50} = 700\ \mu m$, $batch\ \#2$

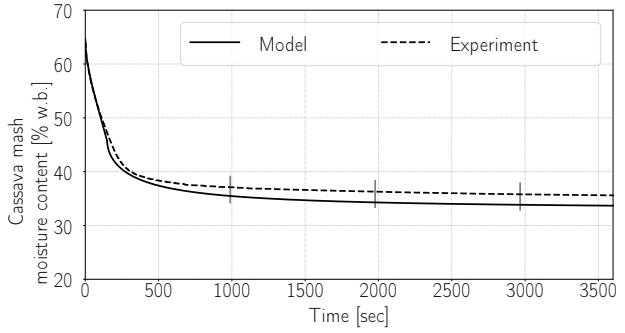

(c) $P = 19\ bar$, $m_0 = 200\ g$, $d_{50} = 1000\ \mu m$, $batch\ \#1$

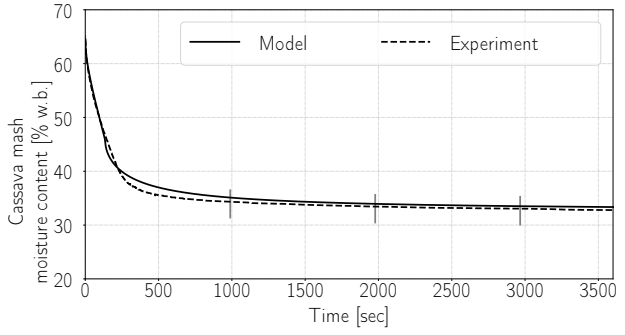

(d) $P = 21\ bar$, $m_0 = 200\ g$, $d_{50} = 700\ \mu m$, $batch\ \#1$

Figure 7: Focus on the first part of cassava mash dewatering kinetics.

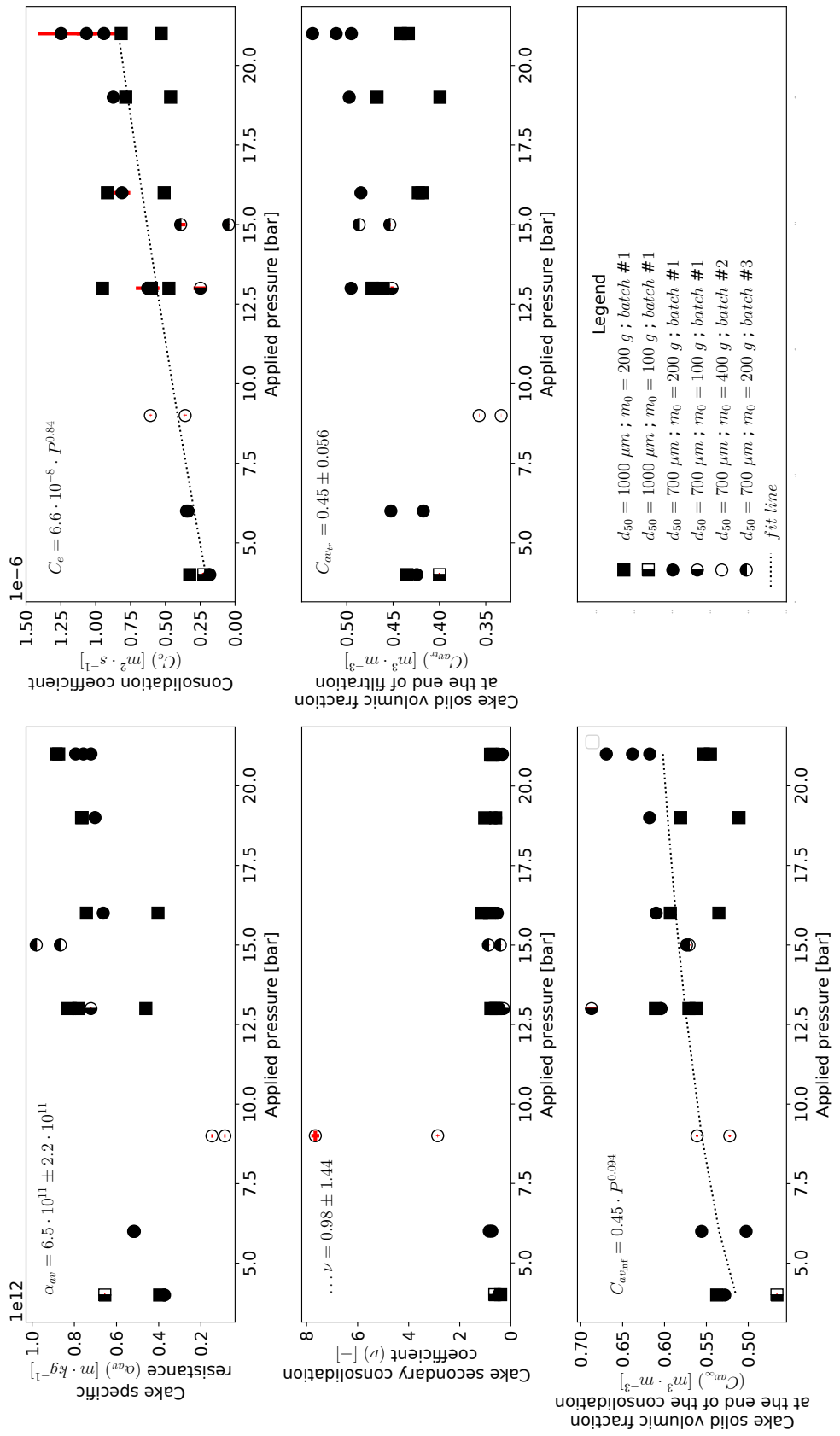

Figure 8: Characteristics of cassava mash in filtration and consolidation: relation to pressure.

List of Tables

1 Preparation and use of the three batches of cassava roots. 30

2 Correlations between the intrinsic characteristics of the product in filtration-consolidation and the applied pressure (Tarleton and Wakeman (2006)). 31

3 Product properties and parameters used in the filtration and consolidation models - origin and values. . 32

4 Errors between model and experiments. 33

5 Summary of all experiments. 34

Table 1
Preparation and use of the three batches of cassava roots.

Experiments on the product allowed either to fit the model, or to evaluate the impact of the deep-freezing on the mash properties.

Batch	d_{50} [μm]		X_0	Conservation at		Model	Freezing
	700	1000	[% $w.b.$]	-15°C[a]	4°C	fitting	impact
#1	×	×	64.7 ± 1.4	×		×	
#2	×		60.5 ± 5.5	×	×	×	×
#3	×		62.3 ± 1.4	×	×	×	×

[a] The product was previously deep-frozen at -25°C.

Table 2
Correlations between the intrinsic characteristics of the product in filtration-consolidation and the applied pressure (Tarleton and Wakeman (2006)).

With P the pressure applied [bar].

Filtration	Specific cake resistance	$\alpha_{av} = \alpha_0 \cdot (1-n) \cdot P^n$
	Volume fraction of solids in cake at the end of filtration	$C_{av_{tr}} = C_{0_{tr}} \cdot P^{\beta_{tr}}$
Consolidation	Volume fraction of solids in cake at the end of consolidation	$C_{av_\infty} = C_{0_\infty} \cdot P^{\beta_\infty}$
	Modified consolidation coefficient	$C_e = C_{e0} \cdot P^{\gamma}$
	Secondary consolidation coefficient	$\nu = \nu_0 \cdot P^{\delta}$

Table 3
Product properties and parameters used in the filtration and consolidation models - origin and values.

Origin	Parameter	Value	Unit
Literature	Dry cassava density ρ_s (Escobar et al. (2018))	1562	$kg \cdot m^{-3}$
	Water density ρ_w	997	$kg \cdot m^{-3}$
	Water viscosity μ_w	$1 \cdot 10^{-3}$	$Pa \cdot s$
Hypothesis	Filter cloth resistance R_s	0	m^{-1}
Equipment characteristics	Drainage surface number i	1	–
	Filtration surface area A	$2.4 \cdot 10^{-3}$	m^2
Measured for each trial	Initial height of product L_0	–	m
	Initial mass of product m_0	–	kg
	Initial moisture content X_0	–	–
	Applied pressure P	–	Pa or bar*
Identified by curve fitting	Specific cake resistance to filtration α_{av}	–	$m \cdot kg^{-1}$
	Volume fraction of solids in cake at the end of the filtration $C_{av_{tr}}$	–	–
	Volume fraction of solids in cake at the end of the consolidation C_{av_∞}	–	–
	Modified consolidation coefficient C_e	–	$m^2 \cdot s^{-1}$
	Secondary consolidation coefficient ν	–	–

* *Depending on the context*

Table 4
Errors between model and experiments.

Errors between the final dry matter content of the cake (DM_∞) predicted by the model and experimentally measured.

Root Mean Squared Error (RMSE) on the cake moisture content (X_{cake}) evaluated all along the experiment.

The average and maximal values and the proportion of experiments for which the prediction error is above 16% are presented.

	Mean	Max	Proportion of trials > 16%
RMSE on X_{cake}	13%	91%	14%
Error on DM_∞	5%	36%	7%

Table 5
Summary of all experiments.

With P the applied pressure; d_{50} the median diameter: M corresponds to a d_{50} of $700\mu m$, G to one of $1000\mu m$; m_0 the initial mass of mash; DM_0, DM_∞, DM_{filt} respectively the dry matter content of the mash before and after dewatering, and of the filtrate;

ID the experiments used to identify the parameters of the correlations between the characteristics of the product and the applied pressure (Table 2).

P [bar]	Batch	d_{50}	m_0 [g]	Dry matter content (w.b.)			Mass balance error [g]	ID
				DM_0	DM_∞	DM_{filtr}		
4	2	M	200.9	31.3%	57.8%	3.6%	0.2	
4	1	M	200.7	36.2%	59.0%	5.6%	2.2	×
4	1	G	200.1	36.0%	60.1%	5.6%	1.3	×
4	1	G	200.0	36.3%	56.2%	5.8%	9.2	
4	1	G	101.0	36.6%	57.5%	5.5%	0.4	×
4	1	G	100.8	36.6%	54.9%	5.5%	3.7	
6	1	M	201.7	36.4%	58.8%	4.3%	1.5	×
6	1	M	201.7	35.5%	59.3%	5.6%	2.3	×
6	1	G	201.7	34.9%	57.2%	5.5%	0.6	
6	1	M	101.6	34.9%	60.5%	5.7%	3.1	
6	1	G	101.0	35.3%	57.4%	5.9%	2.3	
9	2	M	401.4	42.8%	64.3%	8.7%	1.9	
9	2	M	401.3	42.3%	62.0%	9.7%	4.2	×
9	2	M	402.6	41.7%	61.3%	9.3%	5.4	×
9	1	M	201.7	36.9%	59.3%	5.5%	-1.8	
13	1	M	200.8	31.8%	62.9%	5.9%	2.8	
13	1	M	200.3	35.6%	63.1%	5.8%	1.1	
13	1	M	100.8	33.9%	62.5%	5.7%	4.6	×
13	1	M	100.8	31.2%	62.6%	5.7%	4.6	
13	1	G	200.4	34.6%	61.1%	5.6%	1.9	×
13	1	G	200.9	34.6%	60.8%	5.7%	5.9	×
13	1	M	201.1	36.2%	63.0%	6.0%	2.0	×
13	1	G	200.6	35.9%	65.3%	5.7%	0.7	×
15	3	M	201.2	37.4%	62.8%	8.8%	2.5	×
15	3	M	201.2	36.5%	65.7%	4.2%	1.7	×
15	3	M	200.2	39.2%	66.5%	8.3%	4.0	
16	1	M	200.0	35.7%	64.5%	5.7%	1.6	×
16	1	G	201.6	35.7%	65.1%	5.7%	4.3	×
16	1	G	201.6	35.6%	65.9%	5.9%	3.9	×
19	1	M	200.3	35.0%	65.8%	7.8%	4.2	
19	1	M	200.2	37.6%	66.4%	6.0%	3.5	×
19	1	G	200.2	35.4%	64.5%	5.8%	3.5	×
19	1	G	199.9	32.3%	66.8%	5.7%	1.8	×
21	1	M	199.8	35.8%	67.5%	4.5%	4.4	
21	1	M	199.8	35.4%	65.3%	4.5%	2.6	×
21	1	G	201.7	36.0%	65.5%	5.6%	3.7	
21	1	G	199.5	35.0%	65.3%	5.8%	5.5	×
21	1	M	200.4	37.6%	66.1%	5.7%	1.3	×
21	1	G	200.4	33.6%	64.1%	5.8%	2.3	×
21	1	G	200.7	34.4%	67.0%	5.8%	1.6	
21	1	M	201.7	35.4%	67.0%	5.8%	3.5	×